The extra domain A of fibronectin is essential for allergen-induced airway fibrosis and hyperresponsiveness in mice

Martin Kohan, MSc,[a] Andres F. Muro, PhD,[b] Reem Bader, MSc,[a] and Neville Berkman, MBBCh, FRCP[a] *Jerusalem, Israel, and Trieste, Italy*

Background: Asthma is characterized by airway inflammation, airway remodeling, and airway hyperresponsiveness (AHR). Myofibroblast differentiation and subepithelial fibrosis are key features of airway remodeling. Extra domain A (EDA)–containing fibronectin (EDA-FN), an alternatively spliced form of the extracellular matrix protein fibronectin, has been implicated in fibroblast differentiation during wound healing and tissue fibrosis.
Objectives: We sought to investigate the role of EDA-FN in airway remodeling using a murine model of chronic allergen-induced experimental asthma.
Methods: EDA$^{-/-}$ and wild-type (WT) mice were sensitized and exposed to inhaled ovalbumin (OVA) or saline for 5 weeks. EDA-FN expression was evaluated by means of PCR and immunostaining. Peribronchial fibrosis, smooth muscle area, mucus-producing cell numbers, bronchoalveolar cell counts, and lung function were assessed in WT and EDA$^{-/-}$ mice. Fibroblast activation and differentiation were evaluated *ex vivo* by using OVA-treated WT and EDA$^{-/-}$ lung fibroblasts.
Results: Exposure to OVA increased EDA-FN expression in lung tissue and primary lung fibroblasts. OVA-treated EDA$^{-/-}$ mice showed reduced airway fibrosis and AHR and impaired expression of TGF-β1 and IL-13 without changes in airway inflammation or other aspects of remodeling. Lung fibroblasts from OVA-treated EDA$^{-/-}$ mice exhibited reduced proliferation, migration, α-smooth muscle actin expression, and collagen deposition and impaired TGF-β1 and IL-13 release compared with that seen in WT mice.
Conclusions: EDA-FN is essential for the development of OVA-induced airway fibrosis and AHR. The effect of the EDA domain on airway fibrosis after OVA challenge is through activation and differentiation of fibroblasts. Fibroblast activation and airway fibrosis are necessary for the development of AHR. (J Allergy Clin Immunol 2011;127:439-46.)

Key words: *Airway remodeling, asthma, EDA-containing fibronectin, fibroblast, fibrosis, myofibroblast*

Asthma is a chronic disease characterized by airway obstruction, airway hyperresponsiveness (AHR), inflammation, and remodeling.[1] Airway remodeling is defined as changes in the size, mass, or number of structural components of the airway wall, including epithelial disruption, goblet cell hyperplasia and mucus production, subepithelial fibrosis, myofibroblast accumulation, smooth muscle hyperplasia and hypertrophy, and neovascularity.[2-4] The poor response to corticosteroid treatment seen in patients with severe refractory asthma might be due to the presence of remodeling with development of fixed airway obstruction, worsening AHR, and progressive decrease in lung function.[1,5]

The subepithelial fibrosis observed in chronic asthmatic airways is composed of excessive deposition of extracellular matrix (ECM) proteins, such as collagens I, III, and V; fibronectin; tenascin; and laminin.[6-8] Accumulation of fibroblasts/myofibroblasts has been observed in the airways of patients with chronic asthma[9-12] and in the lungs of mice chronically exposed to ovalbumin (OVA).[13] Because myofibroblasts are a major source of collagens and glycoproteins,[2,8] they might account for the enhanced ECM deposition and subepithelial fibrosis observed in patients with chronic asthma.[10,12]

Fibronectin is a 440-kd dimeric major ECM glycoprotein that includes 3 different types of repeating segments (types I, II, and III) and plays a regulatory role during embryogenesis, wound healing, and maintenance of tissue integrity.[14] The fibronectin gene encodes 15 type III repeats that are constitutively expressed plus 2 that are alternatively spliced: extra domain A (EDA) and extra domain B (EDB).[15] EDA is a single exon that is included or excluded from the fibronectin mRNA by exon skipping.[15,16] Two major forms of fibronectin exist: plasma fibronectin, a soluble form found in plasma secreted by hepatocytes, which lacks both EDA and EDB segments, and cellular fibronectin, a form found mainly as fibrils in the ECM and secreted by activated fibroblasts that contains variable proportions of EDA segments, EDB segments, or both.[14-16]

The biological functions of the EDA domain are poorly understood. Inclusion of EDA in fibronectin occurs during wound healing,[16] tissue fibrosis,[17,18] and fibroblast differentiation.[19,20] The changes observed in its pattern of expression during these pathophysiological conditions suggest a role for the EDA domain in fibrogenesis and tissue repair. Increased EDA-containing FN (EDA-FN) levels have been reported in fibroblasts isolated from bronchoalveolar lavage (BAL) fluid of asthmatic patients,[21] in BAL fluid of atopic subjects after allergen bronchoprovocation,[22] and in BAL fluid of OVA-treated mice[23]; however, whether

From [a]the Institute of Pulmonology, Hadassah-Hebrew University Medical Center, Jerusalem, and [b]the International Centre for Genetic Engineering and Biotechnology, Trieste.

Supported by grants from the Israel Science Foundation (1408/08) and the Chief Scientist Office of the Ministry of Health, Israel (4921) to N.B.
Disclosure of potential conflict of interest: The authors have declared that they have no conflict of interest.
Received for publication July 8, 2010; revised October 20, 2010; accepted for publication October 20, 2010.
Available online December 17, 2010.

Reprint requests: Neville Berkman, MBBCh, FRCP, Institute of Pulmonology, Hadassah-Hebrew University Medical Center, POB 12000, Jerusalem, Israel 91120. E-mail: Neville@hadassah.org.il.

0091-6749/$36.00

doi:10.1016/j.jaci.2010.10.021

Abbreviations used
AHR: Airway hyperresponsiveness
α-SMA: α-Smooth muscle actin
ASM: Airway smooth muscle
BAL: Bronchoalveolar lavage
Ct: Cycle threshold
ECM: Extracellular matrix
EDA: Extra domain A
EDA-FN: EDA-containing fibronectin
EDB: Extra domain B
IOD: Integrated optical density
OVA: Ovalbumin
PAS: Periodic acid–Schiff
RGD: Arginyl-glycyl-aspartate
WT: Wild-type

EDA-FN contributes to the development of allergen-induced airway remodeling has not been evaluated. In the present study we used $EDA^{-/-}$ mice to demonstrate that EDA-containing fibronectin is not only upregulated in response to OVA but also is essential for the development of airway fibrosis and AHR.

METHODS

Animals

$EDA^{-/-}$ mice have been previously described.[16] C57BL/6 WT mice were purchased from Harlan Laboratories Ltd (Jerusalem, Israel). The Hebrew University–Hadassah Medical School Animal Ethics Committee approved all experimental protocols. Eight to 9 mice per group were used.

Allergen challenge protocol

Mice were sensitized with intraperitoneal OVA (Sigma-Aldrich, St Louis, Mo) or saline and challenged as previously reported and shown in this article's Fig E1 in the Online Repository at www.jacionline.org.[24,25] Detailed methodology is described in the Methods section of this article's Online Repository at www.jacionline.org.

Assessment of AHR

Twenty-four hours after the last challenge, mice were anesthetized, tracheostomized, paralyzed, and ventilated with FlexiVent (SCIREQ, Montreal, Quebec, Canada). After baseline determination of airway resistance, mice were challenged with 0 to 32 mg/mL methacholine (Spectrum Chemicals, New Brunswick, NJ) nebulized directly into the ventilatory circuit using an AeroNebLab nebulizer (SCIREQ). Two models of respiratory mechanics were used to assess lung resistance: the linear first-order single compartment model and the constant-phase model.[26] All data points were collected with FlexiVent software (SCIREQ). Results were expressed as reative increase over baseline values.

BAL fluid and lung pathology

Murine BAL fluid and lung pathology were processed as previously described,[24,25] and details are provided in the Methods section of this article's Online Repository.

PCR

Quantitative real-time PCR analysis was performed as previously described.[24] The methodology is detailed in the Methods section of this article's Online Repository.

Immunohistochemistry

Slides were processed as previously described.[24,25] The detailed protocol is presented in the Methods section of this article's Online Repository.

Determination of lung collagen content, peribronchial smooth muscle area, and mucus-producing cells

Lung collagen content, area of α-smooth muscle actin (α-SMA) immunostaining, and number of periodic acid–Schiff (PAS)–positive bronchial epithelial cells were determined as previously reported,[25] and details are described in the Methods section of this article's Online Repository.

ELISA

ELISAs for TGF-β1, IL-4, IL-13, and GM-CSF were performed in lung tissue homogenates and fibroblast culture medium by using commercial kits (R&D systems, Minneapolis, Minn, or PeproTech Asia, Rehovot, Israel), as previously described,[20,25] and details are presented in the Methods section of this article's Online Repository.

Lung fibroblast isolation and culture

Cells were isolated from lungs as detailed in the Methods section of this article's Online Repository and as previously described.[20,25] Cells between passages 2 and 4 were used for all experiments. Experiments were repeated 4 times.

Fibroblast proliferation and migration assays

Cell proliferation and migration were determined as previously described.[25] Further details appear in the Methods section of this article's Online Repository.

Immunofluorescence for α-SMA

Fibroblasts were prepared, incubated with anti-mouse α-SMA (Sigma), examined, and analyzed as previously described[20,25] and as detailed in the Methods section of this article's Online Repository. Results are expressed as integrated optical density (IOD).

Collagen deposition by cultured fibroblasts and collagen gel contraction assay

Collagen deposition and 3-dimensional gel contraction were determined as previously described.[20,25,27] Further details appear in the Methods section of this article's Online Repository.

Data analysis

Means and SEMs are given for each group. Statistical analysis was performed with GraphPad Prism software (GraphPad Software, Inc, La Jolla, Calif).[16,20,25] The unpaired Student *t* test (Fig 1, *A* and *B*) and 2-way ANOVA followed by the Bonferroni posttest (Figs 2, 3, 4, and 5, *A* and *B*) were used for sample sizes of 8 to 9. For sample sizes of 4 (Figs 1, *E*; 5, *C* and *D*; and 6), group comparisons were performed by using the nonparametric Kruskal-Wallis test, and 2-group comparisons were performed with the Mann-Whitney test. A P value of less than .05 was considered statistically significant.

RESULTS

Expression of EDA-FN in lung tissue and primary lung fibroblasts from OVA-treated mice

To test whether the remodeling changes observed in our model of chronic asthma[24,25] are associated with the upregulation of the EDA segment of fibronectin, we determined the expression of EDA-FN and total fibronectin (EDA-containing and EDA-lacking forms of fibronectin) in lung tissue of mice exposed to OVA and saline. Quantitative real-time PCR revealed a significant increase in mRNA of fibronectin containing the EDA segment in

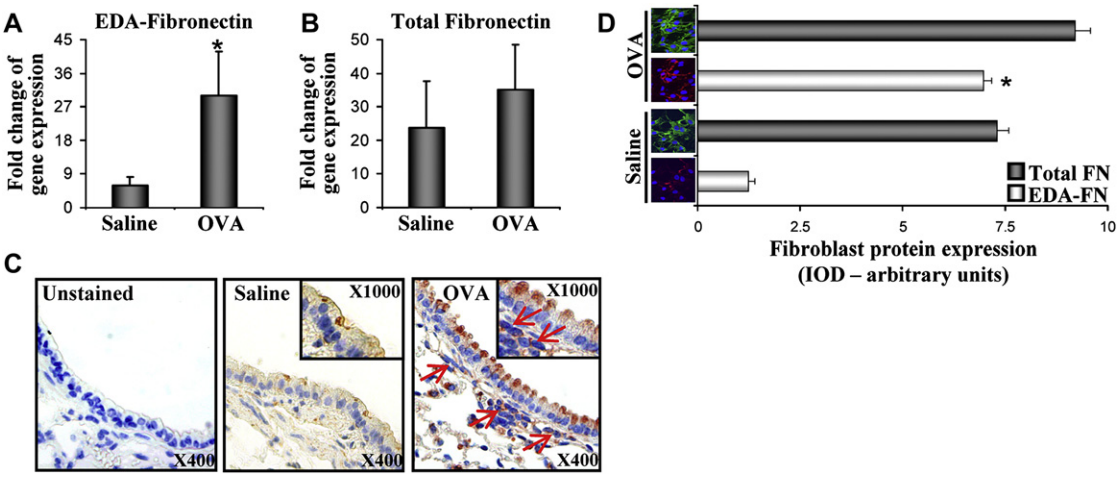

FIG 1. EDA-FN is expressed in lung tissue and fibroblasts from OVA-treated mice. **A** and **B**, EDA-FN (Fig 1, *A*) and total fibronectin (Fig 1, *B*) mRNA in lungs of OVA-treated and control mice (n = 8-9). **P* < .05. **C**, EDA-FN immunostaining of epithelium and subepithelial fibroblasts *(arrows)* in lung sections of OVA-treated mice. Representative images are shown; *inserts* indicate higher magnification. **D**, EDA-FN (*red panels, light bars*) and total fibronectin (*green panels, dark bars*) expression, calculated as integrated optical density *(IOD)*, in lung primary fibroblasts (n = 4). **P* < .05.

lungs of OVA-treated mice in comparison with that seen in saline-treated control animals (Fig 1, *A*; $P < .05$), whereas the increase in total fibronectin mRNA levels was not significant (Fig 1, *B*). The upregulation of EDA-FN mRNA was accompanied by an increase in EDA-FN protein levels in epithelial cells and fibroblasts in lung sections of OVA-treated mice, as demonstrated by means of EDA-FN immunostaining, which was semiquantified as detailed in the Online Repository (Fig 1, *C*, and Fig E2, *A* in this article's Online Repository at www.jacionline.org). Increased expression of EDA-FN was also observed in primary fibroblasts isolated from the lungs of mice exposed to OVA (6.9 ± 0.2 units for OVA vs 1.2 ± 0.2 units for saline, $P < .05$; Fig 1, *D*). Although total FN expression in both OVA and saline-treated cells was similar, most of the fibronectin expressed by OVA-treated lung fibroblasts includes the EDA segment (62% for OVA vs 17% for saline) while this in not so for saline.

AHR is attenuated in EDA$^{-/-}$ mice

AHR is a major clinical feature of asthma.[3,5] We investigated the contribution of EDA-FN to allergen-induced AHR by assessing lung resistance, Newtonian resistance, and tissue damping after methacholine challenge in EDA$^{-/-}$ and WT mice exposed to OVA or saline. OVA-treated WT mice demonstrated increased lung resistance, Newtonian resistance, and tissue damping in comparison with that seen in saline-treated control animals. OVA-treated EDA$^{-/-}$ mice exhibited decreased lung resistance (Fig 2, *A*; $P < .05$), Newtonian resistance (Fig 2, *B*; $P < .01$), and tissue damping (Fig 2, *C*; $P < .05$) in comparison with that seen in OVA-treated WT mice.

Airway inflammation is unchanged in EDA$^{-/-}$ mice in response to acute or chronic allergen challenge

We analyzed the number of total cells and eosinophils in BAL fluid of EDA$^{-/-}$ and WT mice to determine whether EDA-FN influences airway inflammation. An increased number of total cells and eosinophils was observed in both EDA$^{-/-}$ and WT mice exposed to OVA for 1 week (acute challenge; Fig 3, *A* and *C*) and 5 weeks (chronic challenge; Fig 3, *B* and *D*) in comparison with that seen in saline-treated control animals. In comparison with WT mice, EDA$^{-/-}$ mice showed no differences in the number of total cells or eosinophils after 1 week (Fig 3, *A* and *C*) or 5 weeks (Fig 3, *B* and *D*) of OVA challenge. Hematoxylin and eosin–stained lung sections from OVA-treated EDA$^{-/-}$ and WT mice showed similar perivascular and peribronchial inflammatory infiltrates (data not shown).

Reduced subepithelial fibrosis and collagen deposition in EDA$^{-/-}$ mice

To determine whether EDA-FN plays a role in the development of airway remodeling, we evaluated collagen deposition and subepithelial fibrosis, airway smooth muscle (ASM) mass, and goblet cell numbers in OVA-treated EDA$^{-/-}$ and WT mice. Collagen deposition was evaluated by using a biochemical assay, and subepithelial fibrosis was evaluated by means of peribronchial Masson trichrome staining. OVA-treated EDA$^{-/-}$ mice showed reduced lung collagen content compared with that seen in WT mice (149.2 ± 13.9 μg/100 mg of lung tissue for EDA$^{-/-}$ mice vs 258.3 ± 15.2 μg/100 mg of lung tissue for WT mice, $P < .01$; Fig 4, *A*). Peribronchial collagen area, assessed by using Masson trichrome staining and semiquantitative scoring (see the Methods section of this article's Online Repository), was also reduced in lung OVA-treated EDA$^{-/-}$ mice (Fig 4, *B*, and Fig E2, *B*). ASM thickness was evaluated by means of α-SMA immunostaining. OVA challenge increased α-SMA–stained peribronchial smooth muscle area in WT and EDA$^{-/-}$ mice in comparison with saline controls (Fig 4, *C* and *D*); however, no differences were observed between OVA-treated EDA$^{-/-}$ mice (4.9 ± 0.4 $\mu m^2/\mu m$ perimeter of bronchus) and WT mice (4.7 ± 0.4 $\mu m^2/\mu m$ perimeter of bronchus; Fig 4, *C*). Lung sections of WT and EDA$^{-/-}$ mice exposed to OVA showed increased number of PAS-positive epithelial cells in comparison with that seen in

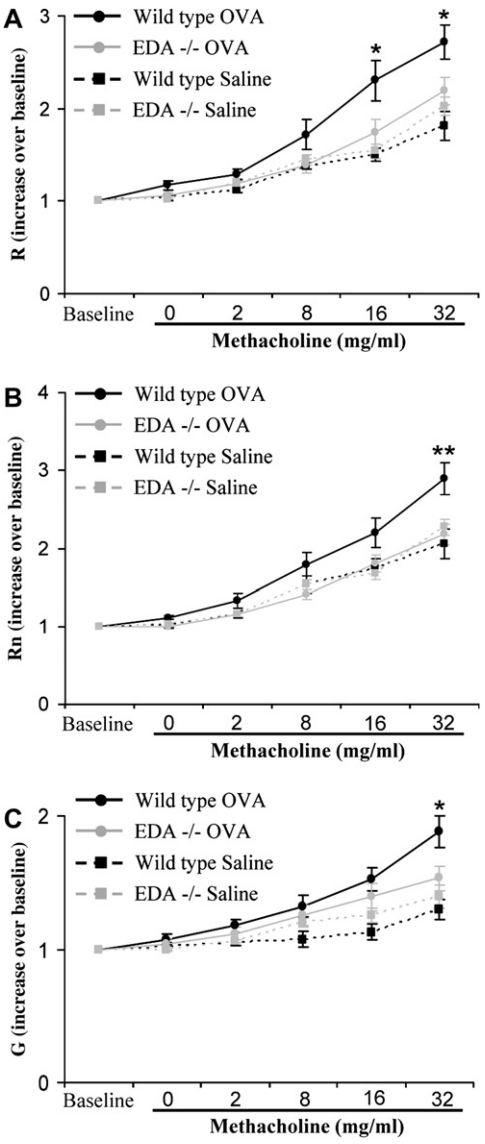

FIG 2. Reduced AHR in EDA$^{-/-}$ mice. **A-C**, Lung resistance (*R*; Fig 2, *A*), Newtonian resistance (*Rn*; Fig 2, *B*), and tissue damping (*G*; Fig 2, *C*) for increasing doses of methacholine. OVA-treated EDA$^{-/-}$ mice (*gray circles*, *solid lines*) showed reduced airway responsiveness in comparison with that seen in OVA-treated WT mice (*black circles*, *solid lines*; n = 8-9). **P* < .05, ***P* < .01 (OVA-treated EDA$^{-/-}$ mice vs OVA-treated WT mice).

saline-treated control animals (Fig 4, *E* and *F*). The percentage of PAS-positive epithelial cells observed in sections of OVA-treated EDA$^{-/-}$ mice (16.2% ± 1.9%) was similar to that of OVA-treated WT mice (18.9% ± 1.6%; Fig 4, *E*).

Reduced expression of TGF-β1 and IL-13 in EDA$^{-/-}$ mice

TGF-β1 and IL-13 are important profibrogenic mediators in asthma.[28] The expression of TGF-β1 in lung homogenates from OVA-treated EDA$^{-/-}$ mice was significantly reduced in comparison with that seen in WT mice (0.26 ± 0.02 vs 0.43 ± 0.04 ng/mL TGF-β1, $P < .001$; Fig 5, *A*). We also evaluated the levels of IL-13, IL-4, and GM-CSF in lung homogenates from WT and EDA$^{-/-}$ mice exposed to OVA and saline and observed reduced expression of IL-13 in lungs of OVA-treated EDA$^{-/-}$ mice compared with that seen in WT mice (67 ± 2 vs 103 ± 2 pg/mL IL-13, $P < .001$; Fig 5, *B*). No differences for IL-4 and GM-CSF were observed between EDA$^{-/-}$ and WT mice exposed to OVA (see Fig E3 in this article's Online Repository at www.jacionline.org). Primary lung fibroblasts from OVA-treated WT mice released increased amounts of TGF-β1 (Fig 5, *C*) and IL-13 (Fig 5, *D*) measured in culture medium compared with those seen in saline-treated control animals. This increase was not observed in OVA-treated EDA$^{-/-}$ mice (1.25 ± 0.18 ng/mL of TGF-β1 for WT mice vs 0.45 ± 0.04 ng/mL of TGF-β1 for EDA$^{-/-}$ mice [Fig 5, *C*] and 93.7 ± 11.1 pg/mL IL-13 for WT mice vs 41.6 ± 1.6 pg/mL IL-13 for EDA$^{-/-}$ mice [Fig 5, *D*], $P < .05$).

Impaired fibroblast activation and differentiation in EDA$^{-/-}$ mice

We next evaluated whether the mechanism of action of EDA-FN in OVA-induced airway fibrosis is through alteration of fibroblast phenotype. We therefore measured proliferation, migration, α-SMA expression, collagen deposition, and contractile capacity of fibroblasts. Proliferation of fibroblasts from lungs of OVA-treated EDA$^{-/-}$ mice was reduced in comparison with that seen in WT mice, with maximal effect observed after 3 days of incubation ($4.1 \pm 0.2 \times 10^5$ cells for EDA$^{-/-}$ mice vs $5.9 \pm 0.3 \times 10^5$ cells for WT mice, $P < .05$; Fig 6, *A*). EDA$^{-/-}$ lung fibroblasts exhibited reduced migration in comparison with WT lung fibroblasts after OVA challenge, as determined by percentage of recovered wound area after 16 hours (49.0 ± 3.0 for EDA$^{-/-}$ mice vs 72.0 ± 2.3 for WT mice, $P < .01$; Fig 6, *B*). α-SMA expression in fibroblasts from lungs of OVA-treated EDA$^{-/-}$ mice was reduced in comparison with that seen in fibroblasts from OVA-treated WT mice (1.26 ± 0.17 units vs 2.83 ± 0.24 units, $P < .05$; Fig 6, *C*). OVA-treated EDA$^{-/-}$ fibroblasts showed less collagen deposition than OVA-treated WT cells (7.1% ± 4.3% vs 42.2% ± 5.8% relative to internal controls, as described in the printed Methods section and in the Methods section of this article's Online Repository; $P < .05$; Fig 6, *D*). Fibroblasts from lungs of OVA-treated EDA$^{-/-}$ mice also demonstrated reduced contractile capacity in comparison with that seen in OVA-treated WT cells. After 24 hours of incubation, EDA$^{-/-}$ cells reduced the gel by 24% of its initial size, whereas WT cells reduced the gel by 44% ($P < .05$; Fig 6, *E*).

DISCUSSION

In this study we evaluate the role of EDA-FN in a murine model of chronic allergen-induced experimental asthma.[24,25] We demonstrate that EDA-FN is upregulated in OVA-treated mice. EDA null mice chronically exposed to OVA show reduced subepithelial fibrosis and collagen deposition, as well as reduced AHR, in comparison with WT mice, whereas no differences in airway inflammation, peribronchial smooth muscle area, and mucus-producing cell numbers are observed. We also show reduced proliferation, migration, α-SMA expression, collagen deposition, contractility, and TGF-β1 and IL-13 expression in lung fibroblasts isolated from OVA-treated EDA$^{-/-}$ mice in comparison with that seen in lung fibroblasts from OVA-treated WT mice. We therefore demonstrate an essential and selective role for EDA-FN in the activation of lung fibroblasts and the development of subepithelial fibrosis and AHR in our model.

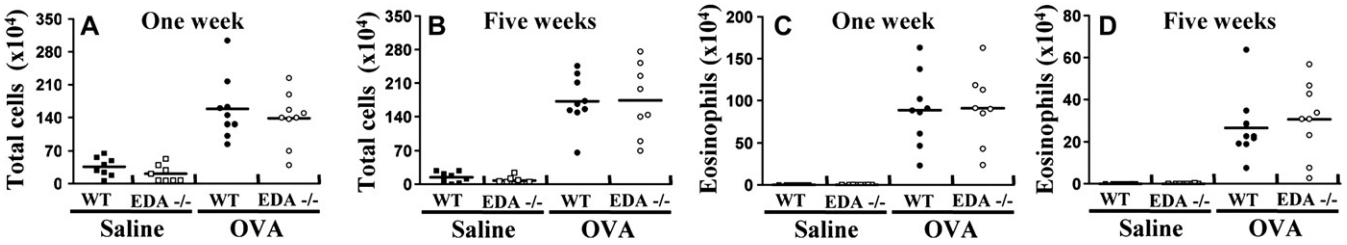

FIG 3. Airway inflammation is unchanged in OVA-treated EDA$^{-/-}$ mice. A similar number of total cells are present in BAL fluid of WT and EDA$^{-/-}$ mice after 1 **(A)** and 5 **(B)** weeks of exposure to OVA. No differences in eosinophils number were observed after 1 **(C)** and 5 **(D)** weeks of OVA treatment. Data are presented as means ± SEMs (n = 8-9).

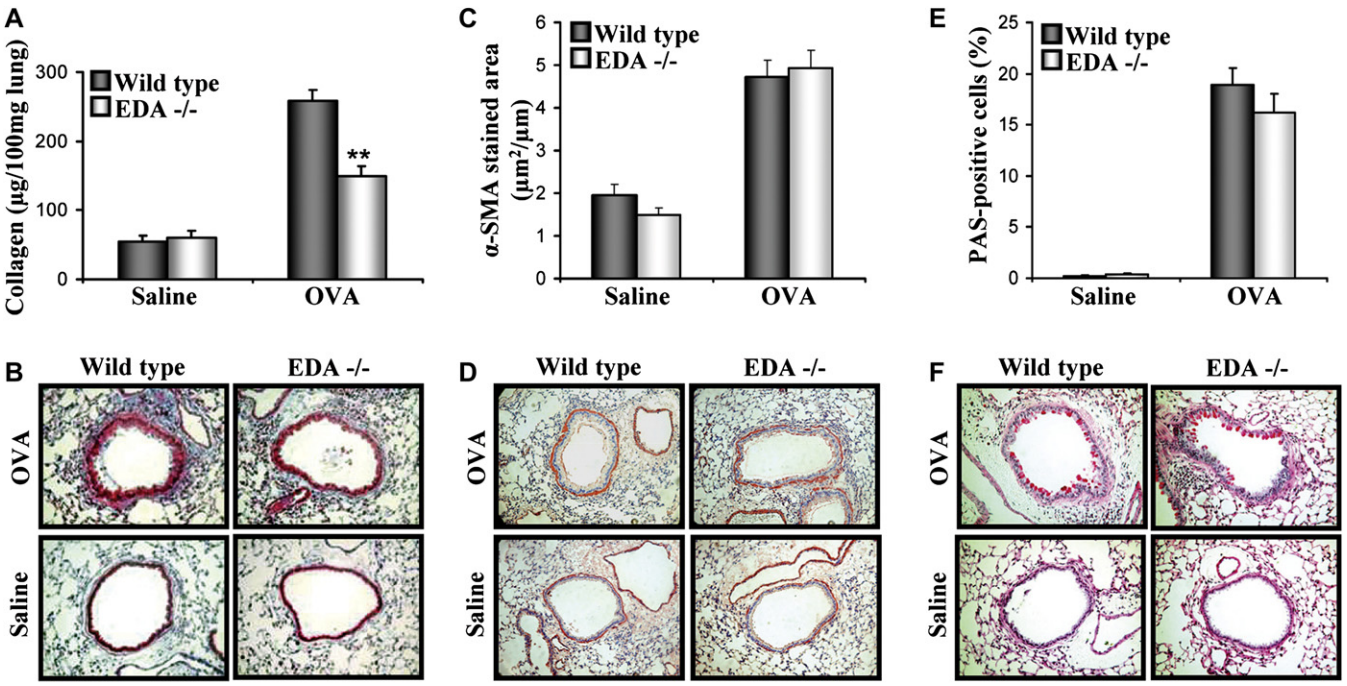

FIG 4. Reduced airway fibrosis in EDA$^{-/-}$ mice. WT and EDA$^{-/-}$ mice were exposed to OVA and saline for 5 weeks. OVA-treated EDA$^{-/-}$ mice showed reduced lung collagen content **(A)** and peribronchial collagen deposition **(B)**. No differences were observed in smooth muscle α-SMA–immunostained area (**C** and **D**) and airway mucus production (**E** and **F**). Data are presented as mean ± SEMs (n = 8-9). $^{**}P < .01$.

We observed increased expression of EDA-FN mRNA and protein, with only a small increase in total fibronectin (EDA-containing and EDA-lacking fibronectin) in both lung tissue and primary lung fibroblasts from OVA-treated mice. Our results are consistent with those of Larsen et al,[21] who found increased EDA-FN expression but no changes in total fibronectin in fibroblasts isolated from BAL fluid of asthmatic patients. Furthermore, Meerschaert et al[22] showed that allergen challenge increased EDA-FN production by airway cells. Together, these findings suggest that allergen challenge induces a shift in fibronectin synthesis from mainly non–EDA-FN to EDA-FN.

AHR is the most important clinical manifestation of asthma and accounts for symptoms and impaired lung function.[3,5] The relationship between AHR, airway inflammation, and individual or combined aspects of airway remodeling are poorly defined. There is ongoing debate regarding the contribution of airway fibrosis, ASM, or both to AHR. We observed that OVA-exposed EDA$^{-/-}$ mice have attenuated AHR in the presence of selective reduction of fibroblast activation and airway fibrosis, demonstrating that these components of remodeling are necessary for the development of AHR in this model. Indeed, our model serves as an excellent tool to specifically evaluate the contribution of fibroblast activation and airway fibrosis to allergen-induced airway diseases. In line with our findings, a strong correlation between subepithelial fibrosis and AHR in response to methacholine or histamine has been reported in asthmatic subjects.[29,30] Others found a correlation between AHR and ECM protein deposition by activated bronchial fibroblasts in asthmatic subjects.[31] Locke et al[32] observed that AHR in mice exposed to OVA for 6 weeks was associated with the development of fibrosis and suggested that airway fibrosis *per se* might be an important factor contributing to AHR, whereas others found no such relationship.[33]

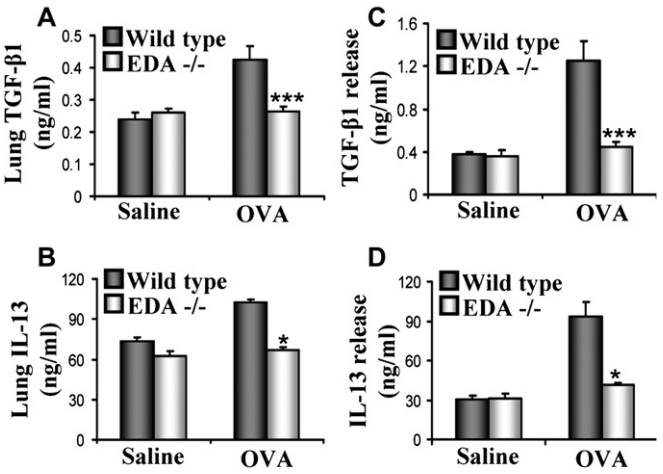

FIG 5. Reduced expression of TGF-β1 and IL-13 in EDA$^{-/-}$ mice. Reduced lung tissue levels of TGF-β1 **(A)** and IL-13 **(B)** are seen in OVA-treated EDA$^{-/-}$ mice (n = 8-9). ***$P < .001$. Reduced release of TGF-β1 **(C)** and IL-13 **(D)** is seen in culture medium from OVA-treated EDA$^{-/-}$ lung fibroblasts after 24 hours of incubation (n = 4). *$P < .05$.

Furthermore, in the classic study of Benayoun et al,[12] they found that the best correlates of asthma severity and reduced lung function are fibroblast accumulation and ASM hypertrophy.

ASM is widely considered to be the major effector of AHR.[34] However, the impaired AHR observed in OVA-treated EDA$^{-/-}$ mice despite the presence of increased ASM area (similar to OVA-treated WT mice) provides evidence that ASM is not the sole contributor to AHR. This is supported by previous studies with murine models of asthma showing increased AHR in the presence of unchanged ASM layer thickness in response to OVA challenge.[32,33] Although unlikely, our findings in this study do not rule out the possibility that EDA-FN might affect AHR through alteration of smooth muscle cell phenotype or behavior without changing smooth muscle content, and this is an interesting focus for further study.

Increased numbers of fibroblasts/myofibroblasts have been reported in the airways of asthmatic subjects, as well as in mice, after chronic exposure to OVA.[9-13] The reduction in airway fibrosis observed in OVA-treated EDA$^{-/-}$ mice is most likely attributable to impaired fibroblast activation and differentiation. EDA-FN promotes migration, proliferation, adhesion, and differentiation of lung fibroblasts and is able to restore profibrotic responses when added to EDA$^{-/-}$ lung fibroblasts.[18,20] EDA-FN might also regulate lung fibroblast activity through modulation of profibrogenic factors. This is supported by our findings showing reduced expression of TGF-β1 and IL-13 *in vivo* from lung tissue of OVA-treated EDA$^{-/-}$ mice, as well as *ex vivo* from cultured fibroblasts isolated from the lungs of these mice. IL-13 production has been described in skin and gingival fibroblasts.[35,36] TGF-β1 and IL-13 are known to activate lung fibroblasts in patients with asthma.[28] We and others have previously shown that EDA-FN not only enhances expression of TGF-β1 from fibroblasts but also is important for its activation.[18-20] In addition, TGF-β1 increases EDA-FN levels in fibroblasts.[37] Thus these mediators might contribute to fibroblast activation through an autocrine loop that is dependent on EDA-FN. The finding of reduced IL-13 levels in lungs and fibroblasts from OVA-treated EDA$^{-/-}$ mice is surprising, especially in the absence of a change in IL-4 levels and in the presence of sustained airway inflammation and mucus production. It is possible that EDA$^{-/-}$ mice have impaired production of IL-13 from fibroblasts but not from other cells, such as epithelial cells[38] or lymphocytes, and further studies are necessary to clarify these issues.

The origin of the increased smooth muscle observed in patients with asthma is not well established. Several hypotheses have been proposed, including the possibility that smooth muscle arises from further differentiation of resident myofibroblasts.[39,40] We observed no changes in ASM in EDA$^{-/-}$ mice despite the impaired fibroblast activation and differentiation shown by these animals in response to OVA. Although this issue is not the main focus of the present study, our findings suggest that continuous differentiation of myofibroblasts might not be a source for increased ASM.

Dekkers et al[41] have recently reported selective reduction of ASM thickness in a model of chronic experimental asthma by blocking the arginyl-glycyl-aspartate (RGD) sequence present on fibronectin and on several other ECM proteins. Interestingly, these authors did not find changes in allergen-induced fibrosis in the presence of the RGD-blocking peptide. Therefore it can be speculated that different portions within the fibronectin molecule might regulate different aspects of remodeling. In response to OVA challenge, the EDA domain might be necessary for the development of airway fibrosis and the RGD domain for smooth muscle hyperplasia. Because the RGD sequence is constitutively expressed in all isoforms of fibronectin,[15] this might provide an explanation for the similar smooth muscle area we observed in both EDA$^{-/-}$ and WT mice.

In the present study we found no changes in eosinophil and total inflammatory cell numbers in EDA$^{-/-}$ mice compared with those seen in WT mice. Because OVA-treated EDA$^{-/-}$ mice have reduced AHR, these results suggest that persistent airway inflammation is unlikely to be a major contributor to AHR. This is consistent with the observation that AHR in asthmatic patients persists despite prolonged treatment with anti-inflammatory medications, such as corticosteroids.[42]

To date, there is no effective therapy for the treatment of airway remodeling. Corticosteroids have potent anti-inflammatory effects, but their efficacy in attenuating remodeling is poorly established.[7,13,42,43] Targeting TGF-β1 might be a logical approach to treat remodeling in asthma[44]; however, this molecule has pleiotropic anti-inflammatory and immune modulatory effects, and the direct blocking of TGF-β1 might be associated with a high risk of side effects, such as autoimmunity and tumorigenesis.[45,46] Our findings suggest that EDA-FN might be an alternative and safer therapeutic target than TGF-β1 for airway fibrosis and for tissue fibrosis in general. EDA-FN is necessary for TGF-β1–induced activation in fibroblasts.[18,19] In contrast to TGF-β1, the expression of EDA-FN is very low in normal adult tissues and is only upregulated after tissue injury.[47] Furthermore, the biological activity of EDA-FN is far more selective than TGF-β1.[15] Finally, the EDA domain might be an easily accessible sequence *in vivo* because targeting of other sequences within the fibronectin molecule has been shown to be feasible.[41,48]

In summary, using EDA$^{-/-}$ mice, we have uncoupled different parameters of airway remodeling and have demonstrated that EDA-FN is essential for the development of airway fibrosis in a model of chronic experimental asthma. In addition, we provide evidence for a direct contribution of increased subepithelial fibrosis to AHR. OVA-treated EDA$^{-/-}$ mice are protected from the

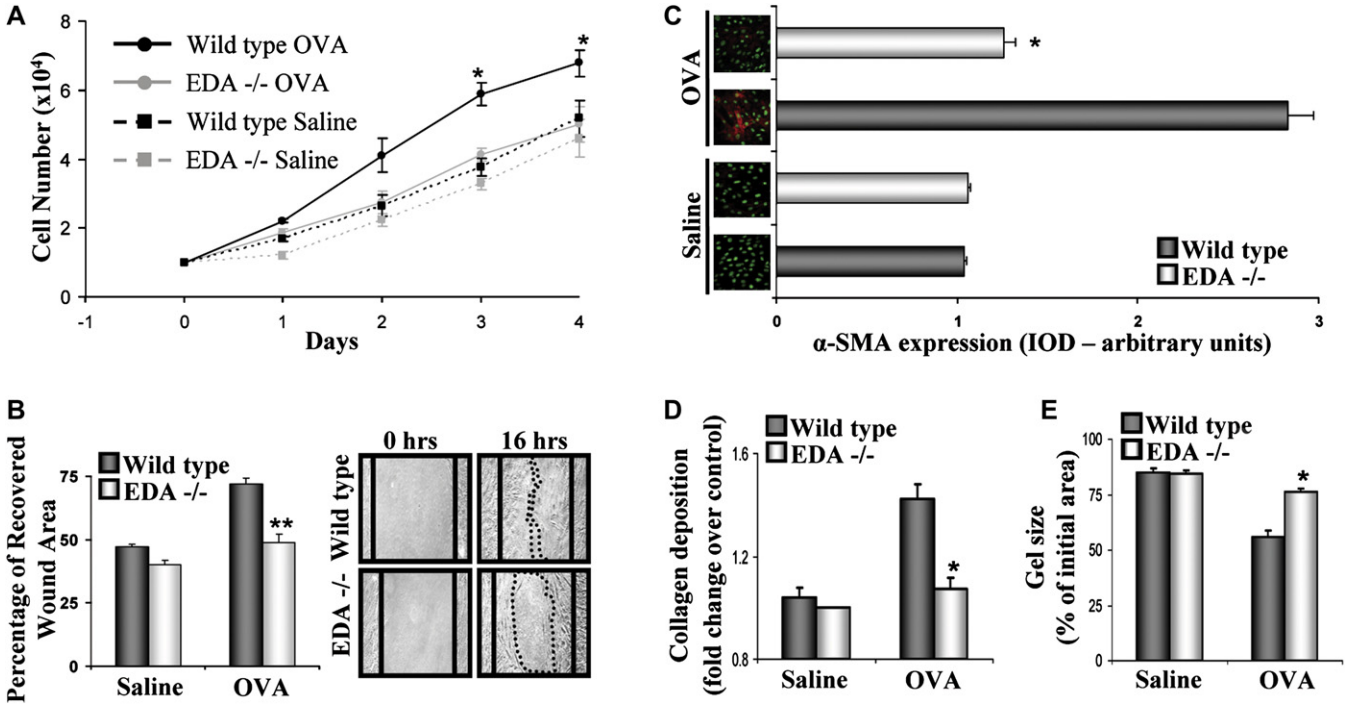

FIG 6. Impaired activation and differentiation of fibroblasts from lungs of OVA-treated EDA$^{-/-}$ mice. Lung fibroblasts from saline- and OVA-treated EDA$^{-/-}$ and WT mice were isolated as described in the printed Methods section and in the Methods section of this article's Online Repository. OVA-treated EDA$^{-/-}$ fibroblasts show reduced proliferation **(A)**, migration **(B)**, α-SMA expression **(C)**, collagen deposition **(D)**, and contractility (**E**; n = 4). *$P < .05$, **$P < .01$.

development of airway fibrosis because of a critical role for EDA-FN in lung fibroblast activation/differentiation, presumably through direct action on lung fibroblasts, through regulation of profibrogenic signals associated to TGF-β1 and IL-13, or both. Thus targeting EDA-FN might be a novel and attractive therapeutic approach to attenuate the development of airway fibrosis and AHR in patients with asthma.

We thank Anita Kol and Golan Buznak (graphic designer) for their technical assistance.

Key messages

- **EDA-FN is essential for the development of OVA-induced airway fibrosis and hyperresponsiveness, and this effect occurs via modulation of myofibroblast phenotype.**
- **Fibroblast activation and airway fibrosis are necessary for the development of AHR.**
- **The use of EDA-FN null mice allows the dissociation and study of different parameters of airway remodeling in response to allergen.**

REFERENCES

1. Tattersfeld AE, Knox AJ, Britton JR, Hall IP. Asthma. Lancet 2002;360:1313-22.
2. Elias JA, Zhu Z, Chupp G, Homer RJ. Airway remodeling in asthma. J Clin Invest 1999;104:985-99.
3. Chiappara G, Gagliardo R, Siena A, Bonsignore MR, Bousquet J, Bonsignore G, et al. Airway remodelling in the pathogenesis of asthma. Curr Opin Allergy Clin Immunol 2001;1:85-93.
4. Jeffery PK. Remodeling in asthma and chronic obstructive lung disease. Am J Respir Crit Care Med 2001;164(suppl):S28-38.
5. Pascual RM, Peters SP. Airway remodeling contributes to the progressive loss of lung function in asthma: an overview. J Allergy Clin Immunol 2005;116:477-86.
6. Laitinen A, Altraja A, Kampe M, Linden M, Virtanen I, Laitinen LA. Tenascin is increased in airway basement membrane of asthmatics and decreased by an inhaled steroid. Am J Respir Crit Care Med 1997;156:951-8.
7. Christie PE, Jonas M, Tsai CH, Chi EY, Henderson WR. Increase in laminin expression in allergic airway remodeling and decrease by dexamethasone. Eur Respir J 2004;24:107-15.
8. Fernandes DJ, Bonacci JV, Stewart AG. Extracellular matrix, integrins and mesenchymal cell function in the airways. Curr Drug Targets 2006;7:567-77.
9. Roche WR, Beasley R, Williams JH, Holgate ST. Subepithelial fibrosis in the bronchi of asthmatics. Lancet 1989;1:520-4.
10. Brewster CEP, Howarth PH, Djukanovic R, Wilson R, Holgate ST, Roche WR. Myofibroblasts and subepithelial fibrosis in bronchial asthma. Am J Respir Cell Mol Biol 1990;3:507-11.
11. Gizycki MJ, Adelroth E, Rogers AV, O'Byrne PM, Jeffery PK. Myofibroblast involvement in the allergen-induced late response in mild atopic asthma. Am J Respir Cell Mol Biol 1997;16:664-73.
12. Benayoun L, Druilhe A, Dombret MC, Aubier M, Pretolani M. Airway structural alterations selectively associated with severe asthma. Am J Respir Crit Care Med 2003;167:1360-8.
13. Miller M, Cho JY, McElwain K, McElwain S, Shim JY, Manni M, et al. Corticosteroids prevent myofibroblast accumulation and airway remodeling in mice. Am J Physiol Lung Cell Mol Physiol 2006;290:L162-9.
14. Hynes RO. Fibronectins 1st ed. In: Springer's Series in Molecular Biology, Rich A, editor. New York: Springer-Verlag; 1990. p. 546.
15. White ES, Baralle FE, Muro AF. New insights into form and function of fibronectin splice variants. J Pathol 2008;216:1-14.
16. Muro AF, Chauhan AK, Gajovic S, Iaconcig A, Porro F, Stanta G, et al. Regulated splicing of the fibronectin EDA exon is essential for proper skin wound healing and normal lifespan. J Cell Biol 2003;162:149-60.
17. Jarnagin WR, Rockey DC, Koteliansky VE, Wang SS, Bissell DM. Expression of variant fibronectins in wound healing: cellular source and biological activity of the EIIIA segment in rat hepatic fibrogenesis. J Cell Biol 1994;127:2037-48.

18. Muro AF, Moretti FA, Moore BB, Yan M, Atrasz RG, Wilke CA, et al. An essential role for fibronectin extra type III domain A in pulmonary fibrosis. Am J Respir Crit Care Med 2008;177:638-45.
19. Serini G, Bochaton-Piallat ML, Ropraz P, Geinoz A, Borsi L, Zardi L, et al. The fibronectin domain ED-A is crucial for myofibroblastic phenotype induction by TGF-β1. J Cell Biol 1998;142:872-81.
20. Kohan M, Muro AF, White ES, Berkman N. EDA-containing cellular fibronectin induces fibroblast differentiation through binding to $\alpha_4\beta_7$ integrin receptor and MAPK/Erk 1/2-dependent signaling. FASEB J 2010;24:4502-13.
21. Larsen K, Malmström J, Wildt M, Dahlqvist C, Hansson L, Marko-Varga G, et al. Functional and phenotypical comparison of myofibroblasts derived from biopsies and bronchoalveolar lavage in mild asthma and scleroderma. Respir Res 2006;7:11.
22. Meerschaert J, Kelly EAB, Mosher DF, Busse WW, Jarjour NN. Segmental antigen challenge increases fibronectin in bronchoalveolar lavage fluid. Am J Respir Crit Care Med 1999;159:619-25.
23. Trifilieff A, El-Hashim A, Bertrand C. Time course of inflammatory and remodeling events in a murine model of asthma: effect of steroid treatment. Am J Physiol Lung Cell Mol Physiol 2000;279:L1120-8.
24. Kohan M, Bader R, Puxeddu I, Levi-Schaffer F, Breuer R, Berkman N. Enhanced osteopontin expression in a murine model of allergen-induced airway remodeling. Clin Exp Allergy 2007;37:1444-54.
25. Kohan M, Breuer R, Berkman N. Osteopontin induces airway remodeling and lung fibroblast activation in a murine model of asthma. Am J Respir Cell Mol Biol 2009; 41:290-6.
26. Tomioka S, Bates J, Irvin CG. Airway and tissue mechanics in a murine model of asthma: alveolar capsule vs. forced oscillations. J Appl Physiol 2002;93:263-70.
27. Puxeddu I, Bader R, Piliponsky AM, Reich R, Levi-Schaffer F, Berkman N. The CC chemokine eotaxin/CCL11 has a selective profibrogenic effect on human lung fibroblasts. J Allergy Clin Immunol 2006;117:103-10.
28. Wilson MS, Wynn TA. Pulmonary fibrosis: pathogenesis, etiology and regulation. Mucosal Immunol 2009;2:103-21.
29. Boulet LP, Laviolette M, Turcotte H, Cartier A, Dugas M, Malo JL, et al. Bronchial subepithelial fibrosis correlates with airway responsiveness to methacholine. Chest 1997;112:45-52.
30. Shiba K, Kasahara K, Nakajima H, Adachi M. Structural changes of the airway wall impair respiratory function, even in mild asthma. Chest 2002;122:1622-6.
31. Westergren-Thorsson G, Chakir J, Lafrenière-Allard MJ, Boulet LP, Tremblay GM. Correlation between airway responsiveness and proteoglycan production by bronchial fibroblasts from normal and asthmatic subjects. Int J Biochem Cell Biol 2002; 34:1256-67.
32. Locke NR, Royce SG, Wainewright JS, Samuel CS, Tang ML. Comparison of airway remodeling in acute, subacute and chronic models of allergic airways disease. Am J Respir Cell Mol Biol 2007;36:626-32.
33. Palmans E, Kips JC, Pauwels RA. Prolonged allergen exposure induces structural airway changes in sensitized rats. Am J Respir Crit Care Med 2000;161:627-35.
34. Martin JG, Duguet A, Eidelman DH. The contribution of airway smooth muscle to airway narrowing and airway hyperresponsiveness in disease. Eur Respir J 2000; 16:349-54.
35. Zurita-Salinas CS, Palacios-Boix A, Yáñez A, González F, Alcocer-Varela J. Contamination with Mycoplasma spp. induces interleukin-13 expression by human skin fibroblasts in culture. FEMS Immunol Med Microbiol 1996;15:123-8.
36. Botero JE, Contreras A, Parra B. Profiling of inflammatory cytokines produced by gingival fibroblasts after human cytomegalovirus infection. Oral Microbiol Immunol 2008;23:291-8.
37. Balza E, Borsi L, Allemanni G, Zardi L. Transforming growth factor beta regulates the levels of different fibronectin isoforms in normal human cultured fibroblasts. FEBS Lett 1988;228:42-4.
38. Allahverdian S, Harada N, Singhera GK, Knight DA, Dorscheid DR. Secretion of IL-13 by airway epithelial cells enhances epithelial repair via HB-EGF. Am J Respir Cell Mol Biol 2008;38:153-60.
39. Tomasek JJ, Gabbiani G, Hinz B, Chaponnier C, Brown RA. Myofibroblasts and mechano-regulation of connective tissue remodelling. Nat Rev Mol Cell Biol 2002;3:349-63.
40. Jones RC, Jacobson M. Angiogenesis in the hypertensive lung: response to ambient oxygen tension. Cell Tissue Res 2000;300:263-84.
41. Dekkers BG, Bos IS, Gosens R, Halayko AJ, Zaagsma J, Meurs H. The integrin-blocking peptide RGDS inhibits airway smooth muscle remodeling in a guinea pig model of allergic asthma. Am J Respir Crit Care Med 2010;181:556-65.
42. Boulet LP, Turcotte H, Laviolette M, Naud F, Bernier MC, Martel S, et al. Airway hyperresponsiveness, inflammation, and subepithelial collagen deposition in recently diagnosed versus long-standing mild asthma. Influence of inhaled corticosteroids. Am J Respir Crit Care Med 2000;162:1308-13.
43. Chakir J, Shannon J, Molet S, Fukakusa M, Elias J, Laviolette M, et al. Airway remodeling-associated mediators in moderate to severe asthma: effect of steroids on TGF-beta, IL-11, IL-17, and type I and type III collagen expression. J Allergy Clin Immunol 2003;111:1293-8.
44. McMillan SJ, Xanthou G, Lloyd CM. Manipulation of allergen-induced airway remodeling by treatment with anti-TGF-beta antibody: effect on the Smad signaling pathway. J Immunol 2005;174:5774-80.
45. Shull MM, Ormsby I, Kier AB, Pawlowski S, Diebold RJ, Yin M, et al. Targeted disruption of the mouse transforming growth factor-beta 1 gene results in multifocal inflammatory disease. Nature 1992;359:693-9.
46. Marx J. DNA repair defect tied to mutated TGF-beta receptor gene. Science 1995; 268:1276-7.
47. Chauhan AK, Iaconcig A, Baralle FE, Muro AF. Alternative splicing of fibronectin: a mouse model demonstrates the identity of in vitro and in vivo systems and the processing autonomy of regulated exons in adult mice. Gene 2004;324:55-63.
48. Neri D, Carnemolla B, Nissim A, Leprini A, Querze G, Balza E, et al. Targeting by affinity-matured recombinant antibody fragments of an angiogenesis associated fibronectin isoform. Nat Biotechnol 1997;15:1271-5.

METHODS

Allergen challenge protocols

Animals were sensitized with intraperitoneal OVA (10 μg of OVA/1 mg of $Al(OH)_3$ in 0.5 mL of 0.9% saline; Sigma) or with saline on days 1 and 10. Mice were then challenged with inhaled saline or OVA (2% wt/vol diluted in 0.9% saline) 3 times per week for 1 week (acute challenge) or 5 weeks (chronic challenge), starting on day 15 (Fig E1). For OVA and saline challenges, mice were transferred into a Perspex 30 × 40 × 40–cm box and exposed to saline or OVA administered by means of a Micro Mist Nebulizer (Hudson RCI, Temecula, Calif), feeding directly into the box at a flow rate of 7 L/min for 20 minutes. The box contains additional holes for air circulation.

BAL cell counts

Twenty-four hours after the last challenge (day 19 for acute challenge or day 47 for chronic challenge), mice were anesthetized with 150 μL of pentobarbitone sodium (200 mg/mL; CTS Chemical, Tel Aviv, Israel). A cannula was placed in the trachea through a small transverse incision made in the neck. After the assessment of AHR, BAL was performed with 4 aliquots of 1 mL of warmed 0.9% saline. BAL fluids were centrifuged for 10 minutes at 1,000 rpm, and cell pellets were resuspended in 1 mL of PBS. Aliquots of 100 μL were used for cytospin preparations by using a Shandon Cytospin 3 (Thermo Fisher Scientific, Waltham, Mass) and stained with Diffquik (Dade Diagnostica, Munich, Germany). A total of 200 BAL cells were counted and classified by using a Newbawer Chamber (Marienfeld, Lauda-Königshofen, Germany). Results are expressed as the number of cells per milliliter of BAL fluid.

Lung pathology

After BAL, animals were killed by means of abdominal aortic transection and exsanguination. Thoracotomy was performed, and the right main bronchus was tied. The right lung was removed, snap-frozen in liquid nitrogen, and stored at −80°C for RNA analysis (lower lobe) and for tissue ELISA and collagen content determination (upper lobe). The left lung was fixed by means of intrabronchial infusion with 1 mL of 4% formaldehyde (Biolab, Jerusalem, Israel) and then immersed in fixative for an additional 24 hours. Transverse sections of the left lung were embedded in paraffin. Four- to 6-μm sections were stained with hematoxylin and eosin, Masson trichrome, or PAS by Hadassah Hospital Pathology Service (Jerusalem, Israel) or used for immunostaining.

Quantitative RT-PCR

Total RNA was isolated from murine right lobe lung tissue by using TriReagent (Sigma-Aldrich), according to the protocol supplied by the manufacturer. RNA integrity and purity were analyzed by means of electrophoresis on 1% agarose gel stained with ethidium bromide. RNA was quantitated by means of spectrophotometry and then reverse transcribed to cDNA under standard conditions, according to the manufacturer's recommendations (Promega, Madison, Wis).

Quantitative real-time PCR analysis was performed with the ABI PRISM 7000 Sequence Detection System (Applied Biosystems, Foster City, Calif). The probes and primers used were designed by Applied Biosystems and purchased as TaqMan Gene Expression assays kits (Applied Biosystems). One kit recognizes a sequence within the EDA domain and detects only fibronectin forms that contain the EDA segment (EDA-FN; assay ID: Mm01256733_m1), whereas the second kit recognizes a sequence shared by all forms of fibronectin, both those containing EDA and those lacking EDA (total fibronectin; assay ID: Mm01256735_m1). The housekeeping gene 18S was used as the internal control for sample normalization. Probe sequences are as follows: EDA-containing fibronectin: 5′-AGT CCA CAG CCA TCC CTG CGC CCAC-3′; total fibronectin, 5′-ATC ACT ACT CTG GAG AAT GTT AGCC-3′; and 18S RNA, 5′-TGG AGG GCA AGT CTG GTG CCA GCAG-3′.

For each primer pair, a dilution curve of a positive cDNA sample was included to calculate the efficiency of the amplification. Universal thermal cycling parameters were used for all reactions, with an initial denaturing step at 95°C for 15 seconds followed by annealing/extension at 60°C for 1 minute. Forty cycles were performed, and each sample was amplified in triplicate. The threshold cycle (Ct) was recorded for each sample to reflect the mRNA expression level, and relative quantification was determined by using ΔCt calculated as follows:

$$Ct_{(\text{Target gene})} - Ct_{(\text{18S gene}).}$$

The product is expressed as the fold change of gene expression according to the formula $2^{-\Delta\Delta Ct}$, as previously described.[E1]

Immunohistochemistry

Immunohistochemical staining was performed on 4- to 6-μm paraffinized sections of murine lung tissue. The sections were deparaffinized with xylene (Gadot Lab Supplies Ltd, Netanya, Israel) and washed. After antigen retrieval in citrate buffer (0.01 mol/L, pH 6), slides were treated with 0.2% Triton for 10 minutes. Sections were then immersed in 0.3% H_2O_2 (Sigma) in methanol for 8 minutes to quench endogenous peroxide, washed, and incubated with Beat blocking solution A and B from a Histomouse-SP bulk kit (Zymed Laboratories, South San Francisco, Calif) for 45 and 10 minutes, respectively. Slides were exposed to anti-α-SMA (Sigma) or anti-EDA fibronectin (clone 3E2, Sigma) for 90 minutes at room temperature or overnight at 4°C. Primary antibodies were detected with a Histomouse-SP broad-spectrum (AEC) detection kit (Zymed Laboratories), according to the manufacturer's recommendations. Briefly, sections were first incubated with biotinylated secondary antibody for 30 minutes at room temperature and then with a streptavidin-biotin complex for 10 minutes. Finally, slides were exposed to a substrate chromogen mixture for 10 minutes. The sections were counterstained with hematoxylin.

The area of peribronchial α-SMA immunostaining was outlined and quantified with an Axiolab light microscope (Zeiss, Carl Zeiss, AG, Oberkochen, Germany), a Coolpix 990 camera (Nikon, Tokyo, Japan) and the image analysis software Image ProPlus 6.0 (Media Cybernetics, Inc, Silver Spring, Md), as previously described.[E2] At least 5 bronchi were counted per slide. Results are expressed as the area of α-SMA stained per micrometer of basement membrane of bronchi.

Immunohistochemical staining for EDA-FN was graded semiquantitatively. All slides were examined by 2 reviewers in a random blinded fashion. Five consecutive airways from all groups of mice were categorized according to the abundance of cellular and peribronchiolar EDA-FN staining and assigned numeric scores (0, <10% EDA-FN staining; 1, 10% to 40%; 2, 40% to 70%; and 3, >70%). Results are expressed as the EDA-FN expression score.

Lung collagen content

Total lung collagen content from 100 μg of right upper lung lobe tissue was determined by using the Sircol Collagen Assay kit (Biocolor Ltd, Belfast, Northern Ireland), according to the manufacturer's recommendations. Results were expressed as micrograms of collagen per 100 μg of lung tissue.

Peribronchial collagen content was semiquantitatively graded in Masson trichrome–stained sections. All slides were analyzed by 2 reviewers in a random blinded fashion. Five consecutive airways from all groups of mice were categorized according to the trichrome stain observed around the airways and assigned numeric scores (0, absence of peribronchial trichrome stain; 1, marginal peribronchial trichrome stain; 2, slight increase in peribronchial trichrome stain; 3, increase in trichrome stain in all airways; and 4, dramatically increased stain in all airways), as previously described.[E3] Results are expressed as the trichrome staining score.

Quantification of mucus-producing cells

Lung sections from all groups of mice were stained for PAS to visualize mucus production by airway epithelial cells. The number of PAS-positive and PAS-negative epithelial cells in individual bronchioles was counted to quantitate the level of mucus expression in the airway, as previously described.[E2,E4] Ten bronchioles were counted in each slide. Results are expressed as the percentage of PAS-positive cells per bronchiole, which is calculated from the number of PAS-positive epithelial cells per bronchus divided by the total number of epithelial cells of each bronchiole.

Murine lung fibroblast isolation and culture

Lungs from EDA$^{-/-}$ and WT mice exposed to saline or OVA as detailed above were removed 24 hours after the last inhalation, minced, and incubated in collagenase solution (1 mg/mL in PBS, Sigma) for 45 minutes at 37°C and then passed through BD Falcon cell strainers (BD Biosciences, Bedford, Mass). Cells were washed with PBS and resuspended in RPMI 1640 medium (Sigma) supplemented with 10% heat-inactivated FCS, 100 μg/mL penicillin, 100 mg/mL streptomycin, 25 mmol/L HEPES buffer, 2 mmol/L L-glutamine, 0.1 mmol/L sodium pyruvate, and 1:100 Nonessential Amino Acids Solution 100-Fold Concentrate (all from Biological Industries, Beit Haemek, Israel). Fibroblasts were passaged every 5 days by dissociating the monolayers with mild trypsin solution (Biological Industries) and then reseeding in 75-cm^2 flasks. Fibroblasts between passages 2 and 4 were used for all experiments, which were repeated 4 times.

Fibroblast proliferation assay

Proliferation was determined based on cell counts, as previously described.[E5] Lung primary fibroblasts from all groups (10^5 per well) were seeded in 12-well plates in RPMI 1640 with 10% FCS (Biological Industries) on day 0. On days 1, 2, 3, and 4, cells were trypsinized and counted with a Coulter cell counter (Beckman Coulter, Inc, Fullerton, Calif).

Culture medium after 24 and 48 hours of incubation was collected, centrifuged, and used for ELISA according to the manufacturer's recommendations. Because similar results were obtained after 24 or 48 hours of culture, we show TGF-β1 and IL-13 release after 24 hours of incubation.

Fibroblast migration assay

Migration was determined by using the "scratch-wound" assay, as previously described.[E6] Lung primary fibroblasts from all groups (10^5 per well) were seeded in 12-well plates and incubated (37°C at 5% CO_2) to confluency. A cell-free wound area was then created by scratching the cells with a pipette tip. The time of the scratching wound was designated as time 0, and pictures were taken. The cultures were then allowed to migrate for 16 hours. At the end of migration, another set of pictures of the same region was taken. The area of the wounds was quantified with ImageJ software (National Institutes of Health, Bethesda, Md). The cell-free areas of the wounds at 16 hours after wounding were subtracted from the areas of the wounds at 0 hours (initial area) to calculate the area covered by migrating cells. Results are expressed as a percentage of recovered wound area by using the following formula:

$$\text{Percentage of recovered wound area} = \frac{(\text{Initial area} - \text{Area after 16 hours})}{\text{Initial area}} \times 100$$

Immunofluorescence

Lung primary fibroblasts (10^4 per well) were placed in 24-well plates. After 24 hours, cells were fixed in 75% methanol, permeabilized in 0.2% Triton 100X, and blocked with BSA 1% in PBS.

For EDA-FN and total fibronectin staining, primary fibroblasts isolated from lungs of WT mice exposed to OVA or saline were coincubated with anti-human EDA murine mAb clone 3E2 (Sigma-Aldrich) and rabbit anti-human goat polyclonal antibody (DakoCytomation, Glostrup, Denmark), as previously described.[E7] Binding was detected by using Cy5-conjugated goat anti-mouse and fluorescein isothiocyanate–conjugated donkey anti-rabbit (Jackson ImmunoResearch Laboratories, Inc, West Grove, Pa).

For α-SMA staining, primary lung fibroblasts from all groups were incubated with anti–α-SMA mAb (clone 1A4, Sigma-Aldrich). Binding was detected with Cy5-conjugated goat anti-mouse antibody (Jackson).

Nuclei were counterstained with propidium iodide (Sigma). Negative controls were performed with cells incubated directly with fluorescent antibodies. Cover slips were then mounted on slides and examined with a FluoView FV 300 confocal laser scanning biological microscope (Olympus Corp, Center Valley, Pa). Ten fields were examined per slide. Quantification of fluorescence was assessed with Image-Pro Plus 6.0 software (Media Cybernetics, Inc, Silver Spring, Md). Integrated optical density was automatically calculated from images acquired at a magnification of ×600 and expressed as previously described.[E8,E9]

Percentage of EDA expression was calculated by using the following formula:

$$\text{Percentage of EDA expression} = \frac{\text{IOD EDA-fibronectin}}{\text{IOD total fibronectin}} \times 100$$

Collagen deposition by fibroblasts

Lung primary fibroblasts (5×10^4 per well) were seeded in 24-well plates and left for 48 hours to reach monolayers. Collagen deposited in each well was then stained with the Sircol Collagen Assay kit (Biocolor Ltd), according to the manufacturer's instructions. The amount of collagen was assessed by means of spectrophotometry at 540 nm. Collagen deposition was expressed as the fold increase relative to deposition by lung fibroblasts isolated from saline-treated EDA$^{-/-}$ mice (internal control).

Gel contraction assay

Three-dimensional gel contraction was performed by using collagen matrices as previously described.[E10] Volumes (0.33) of rat tail type I collagen (3 mg/mL in 0.1% acetic acid, Sigma) were mixed with volumes (0.66) of cell suspension (10^4 per gel) in culture medium in the presence of 0.1 mol/L NaOH. The mixture was immediately transferred to 24-well plates and left for 20 minutes at room temperature for the gels to solidify. Additional culture medium was added to the wells, and the gel was gently released. The plates were then incubated (37°C at 5% CO_2), and after 24 hours, gels were photographed, and their size was determined with ImageJ software. Results are expressed as the percentage of gel initial area calculated as follows:

$$\text{Percentage of gel initial area} = \frac{\text{Gel area after 24 hours}}{\text{Gel initial area}} \times 100$$

REFERENCES

E1. Livak KJ, Schmittgen TD. Analysis of relative gene expression data using real-time quantitative PCR and the 2(-Delta Delta C(T)) Method. Methods 2001;25:402-8.

E2. Cho JY, Miller M, Baek KJ, Han JW, Nayar J, Lee SY, et al. Inhibition of airway remodeling in IL-5 –deficient mice. J Clin Invest 2004;113:551-60.

E3. Le Saux CJ, Teeters K, Miyasato SK, Hoffmann PR, Bollt O, Douet V, et al. Down-regulation of caveolin-1, an inhibitor of transforming growth factor-beta signaling, in acute allergen-induced airway remodeling. J Biol Chem 2008;283:5760-8.

E4. Lim DH, Cho JY, Song DJ, Lee SY, Miller M, Broide DH. PI3K gamma-deficient mice have reduced levels of allergen-induced eosinophilic inflammation and airway remodeling. Am J Physiol Lung Cell Mol Physiol 2009;296:210-9.

E5. Sugiura H, Liu X, Duan F, Kawasaki S, Togo S, Kamio K, et al. Cultured lung fibroblasts from ovalbumin-challenged "asthmatic" mice differ functionally from normal. Am J Respir Cell Mol Biol 2007;37:424-30.

E6. Liang CC, Park AY, Guan JL. In vitro scratch assay: a convenient and inexpensive method for analysis of cell migration in vitro. Nat Protoc 2007;2:329-33.

E7. Muro AF, Chauhan AK, Gajovic S, Iaconcig A, Porro F, Stanta G, et al. Regulated splicing of the fibronectin EDA exon is essential for proper skin wound healing and normal lifespan. J Cell Biol 2003;162:149-60.

E8. Asahara T, Chen D, Takahashi T, Fujikawa K, Kearney M, Magner M, et al. Tie2 receptor ligands, angiopoietin-1 and angiopoietin-2, modulate VEGF-induced postnatal neovascularization. Circ Res 1998;83:233-40.

E9. Gupta S, Natarajan R, Payne SG, Studer EJ, Spiegel S, Dent P, et al. Deoxycholic acid activates the c-Jun N-terminal kinase (JNK) pathway via FAS receptor activation in primary hepatocytes: role of acidic sphingomyelinase-mediated ceramide generation in FAS receptor activation. J Biol Chem 2004;279:5821-8.

E10. Ngo P, Ramalingam P, Phillips JA, Furuta GT. Collagen gel contraction assay. Methods Mol Biol 2006;341:103-9.

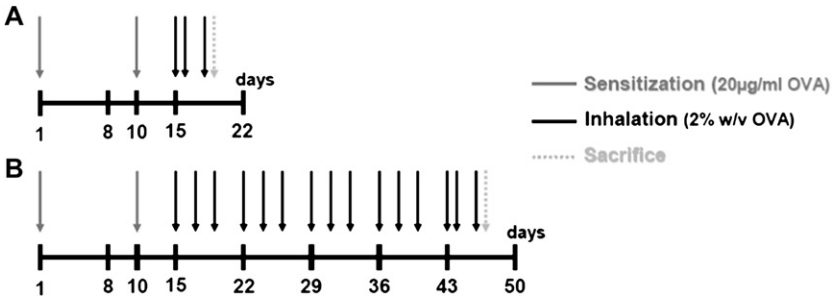

FIG E1. Schematic overview of study protocols for induction of acute **(A)** and chronic **(B)** allergen challenge.

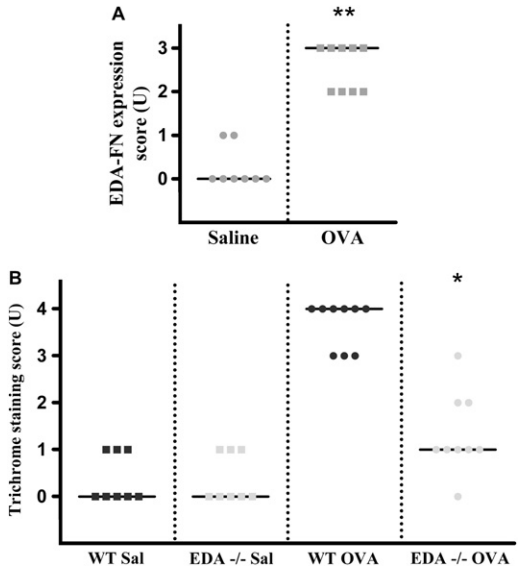

FIG E2. **A**, Lung sections from WT mice challenged with saline *(Sal)* or OVA were immunostained for EDA-FN (see Fig 1, *C*) and assigned an expression score based on the percentage of EDA-FN staining, as described in the Methods section of this article's Online Repository (n = 8-9 per group). $^{**}P < .01$, Mann-Whitney test. **B**, Trichrome-stained lung sections from $EDA^{-/-}$ and WT mice exposed to saline or OVA (see Fig 4, *B*) were assigned a score based on the trichrome staining observed around the airways, as described in the Methods section of this article's Online Repository (n = 8-9 per group). $^{*}P < .05$, WT OVA versus $EDA^{-/-}$ OVA, Kruskal-Wallis/ Dunn test.

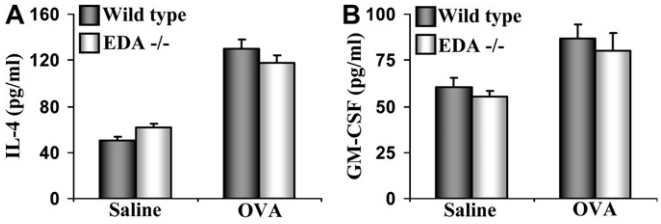

FIG E3. No differences are observed in IL-4 **(A)** and GM-CSF **(B)** levels in lung homogenates from $EDA^{-/-}$ and WT mice exposed to OVA (n = 8-9 per group).